



## University of Groningen

# A discrete solvent reaction field model within density functional theory

Jensen, Lasse; van Duijnen, Piet Th.; Snijders, Jaap G.

Published in: Journal of Chemical Physics

DOI: 10.1063/1.1527010

IMPORTANT NOTE: You are advised to consult the publisher's version (publisher's PDF) if you wish to cite from it. Please check the document version below.

Document Version Publisher's PDF, also known as Version of record

Publication date: 2003

Link to publication in University of Groningen/UMCG research database

Citation for published version (APA): Jensen, L., van Duijnen, P. T., & Snijders, J. G. (2003). A discrete solvent reaction field model within density functional theory. Journal of Chemical Physics, 118(2), 514 - 521. https://doi.org/10.1063/1.1527010

Copyright Other than for strictly personal use, it is not permitted to download or to forward/distribute the text or part of it without the consent of the author(s) and/or copyright holder(s), unless the work is under an open content license (like Creative Commons).

If you believe that this document breaches copyright please contact us providing details, and we will remove access to the work immediately and investigate your claim.

Downloaded from the University of Groningen/UMCG research database (Pure): http://www.rug.nl/research/portal. For technical reasons the number of authors shown on this cover page is limited to 10 maximum.

# A discrete solvent reaction field model within density functional theory

Lasse Jensen, Piet Th. van Duijnen, and Jaap G. Snijders

Citation: J. Chem. Phys. **118**, 514 (2003); doi: 10.1063/1.1527010 View online: https://doi.org/10.1063/1.1527010 View Table of Contents: http://aip.scitation.org/toc/jcp/118/2 Published by the American Institute of Physics

### Articles you may be interested in

A discrete solvent reaction field model for calculating molecular linear response properties in solution The Journal of Chemical Physics **119**, 3800 (2003); 10.1063/1.1590643

A discrete interaction model/quantum mechanical method for simulating surface-enhanced Raman spectroscopy The Journal of Chemical Physics **136**, 214103 (2012); 10.1063/1.4722755

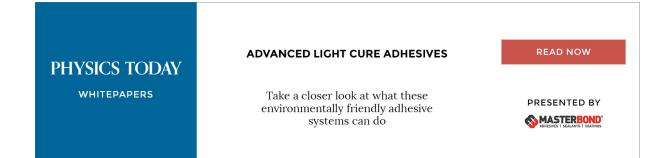
Polarizability of molecular clusters as calculated by a dipole interaction model The Journal of Chemical Physics **116**, 4001 (2002); 10.1063/1.1433747

A discrete interaction model/quantum mechanical method to describe the interaction of metal nanoparticles and molecular absorption The Journal of Chemical Physics **135**, 134103 (2011); 10.1063/1.3643381

A discrete interaction model/quantum mechanical method for describing response properties of molecules adsorbed on metal nanoparticles The Journal of Chemical Physics **133**, 074103 (2010); 10.1063/1.3457365

A consistent and accurate ab initio parametrization of density functional dispersion correction (DFT-D) for the 94 elements H-Pu

The Journal of Chemical Physics 132, 154104 (2010); 10.1063/1.3382344



# A discrete solvent reaction field model within density functional theory

Lasse Jensen,<sup>a)</sup> Piet Th. van Duijnen, and Jaap G. Snijders Theoretical chemistry, Material Science Centre, Rijksuniversiteit Groningen, Nijenborgh 4, 9747 AG Groningen, The Netherlands

(Received 12 September 2002; accepted 15 October 2002)

In this work we present theory and implementation for a discrete reaction field model within Density Functional Theory (DFT) for studying solvent effects on molecules. The model combines a quantum mechanical (QM) description of the solute and a classical description of the solvent molecules (MM). The solvent molecules are modeled by point charges representing the permanent electronic charge distribution, and distributed polarizabilities for describing the solvent polarization arising from many-body interactions. The QM/MM interactions are introduced into the Kohn-Sham equations, thereby allowing for the solute to be polarized by the solvent and vice versa. Here we present some initial results for water in aqueous solution. It is found that the inclusion of solvent polarization is essential for an accurate description of dipole and quadrupole moments in the liquid phase. We find a very good agreement between the liquid phase dipole and quadrupole moments obtained using the Local Density Approximation and results obtained with a similar model at the Coupled Cluster Singles and Doubles level of theory using the same water cluster structure. The influence of basis set and exchange correlation functional on the liquid phase properties was investigated and indicates that for an accurate description of the liquid phase properties using DFT a good description of the gas phase dipole moment and molecular polarizability are also needed. © 2003 American Institute of Physics. [DOI: 10.1063/1.1527010]

### I. INTRODUCTION

An interesting theoretical problem is the modeling of molecular properties in the condensed phase. In general, the interactions with the solvent changes the molecular properties considerably when compared with the gas phase. From a quantum chemical point of view the focus is on a single molecule (or a molecular system) and the solvent effects are treated as perturbations of the molecular system. The molecular system of interest is then treated with a quantum mechanical method and the rest of the system is treated by a much simpler method, usually a classical description.<sup>1–15</sup>

The methods used for the classical description of the solvent can in general be divided into two groups depending on the detail in which the solvent are considered. The first group of methods are the so-called continuum models $^{1-3}$  in which the solvent is treated as a continuous medium characterized by its macroscopic dielectric constants. The continuum models have become a standard approach for modeling solvent effects on molecular properties within computational chemistry and are very efficient models. However, in the continuum model the explicit microscopic structure of the solvent are neglected and therefore provides a poor description of the short range interactions. Also, the results are affected by the choice of the radius and shape of the cavity in which the solute is embedded into.<sup>16</sup> The second group of methods can be characterized as discrete solvent methods where one or more solvent molecules are treated explicitly. Among these methods are the supermolecular model,17 frozen density functional approach,18 ab initio molecular dynamics (MD),<sup>19</sup> and the combined quantum mechanical and classical mechanical models (QM/MM).<sup>4-15</sup> In both the supermolecular models and in ab initio MD models all molecules are treated at the same level of theory. This gives a highly accurate description of the solvent-solute interaction but due to the high computational demand only a few solvent molecules can be included. A problem of these types of models is that there is no unique way of defining properties of the individual molecules.<sup>20–22</sup> The definition of the molecular properties require an arbitrary partitioning of the wave function or the electronic charge density among the molecules much in the same way as defining atomic charges. The molecular properties will depend on the particular partitioning scheme employed as shown in an ab initio MD study<sup>20</sup> of ice Ih, where it was found that the average dipole moment ranges from 2.3 to 3.1 D depending on which partitioning scheme used.

In the QM/MM methods<sup>4–15</sup> the system is divided into a quantum mechanical part, the solute, and a classical part, the solvent, and the interaction between the two subsystems are described with an effective operator. The solvent molecules are then treated with a classical force field and the method therefore allows for a greater number of solvent molecules to be included. Like in the continuum model the solute is separated from the solvent molecules and the molecular properties of the solute are therefore well defined. The remaining problem is finding an accurate approximate representation of the solvent molecules and the solvent molecules introduces a large number of solvent configurations over which the solute properties must be averaged. This is typically done

<sup>&</sup>lt;sup>a)</sup>Author to whom correspondence should be addressed. Electronic mail: l.jensen@chem.rug.nl

using Monte Carlo or MD techniques which lead to a large number of quantum mechanical calculations. For this reason the QM/MM method is often employed at a semiempirical level of theory.<sup>14</sup>

The force field used in the QM/MM methods are typically adopted from fully classical force fields. While this in general is suitable for the solvent–solvent interactions it is not clear how to model the van der Waals interaction between the solute and the solvent.<sup>24</sup> The van der Waals interactions are typically treated as a Lennard-Jones (LJ) potential and the LJ parameters for the quantum atoms are then taken from the classical force field or optimized to the particular QM/MM method<sup>25</sup> for some molecular complexes. However, it is not certain that optimizing the parameters on small complexes will improve the results in a QM/MM simulation<sup>24</sup> of a liquid.

In recent years the classical force fields have been improved in order to also describe the polarization of the molecules.<sup>26–33</sup> The polarization of the classical molecules has also been included in QM/MM studies<sup>4,5,34-40</sup> and shown that it is important to consider also the polarization of the solvent molecules. Since the inclusion of the solvent polarization leads to an increase in computational time most studies ignore this contribution and use the more simple pair potentials. When the solvent polarization is included it is usually treated using either an isotropic molecular polarizability<sup>35,39</sup> or using distributed atomic polarizabilities<sup>34,37,38,40</sup> according to the Applequist scheme.<sup>41</sup> At short distances the Applequist scheme leads to the so-called "polarizability catastrophy" $^{41-43}$  due to the use of a classical description in the bonding region. Thole<sup>43</sup> avoided this problem by introducing smeared out dipoles which mimics the overlapping of the charges distributions at short distances. Thole's model has been shown to be quite successful in reproducing the molecular polarizability tensor using model atomic polarizability parameters independent of the chemical environment of the atoms.<sup>43-45</sup> This model is used in the Direct Reaction Field model<sup>5,11</sup> which is an *ab initio* QM/MM model. However, so far the inclusion of solvent polarization using Thole's model has not been considered within a Density Functional Theory (DFT) approach.

Therefore, in this work we present an implementation of a QM/MM-type model for the study of solvation effect on molecules within DFT. The model will be denoted the Discrete Reaction Field (DRF) model. In the DRF model the discrete solvent molecules are represented by distributed atomic point charges and polarizabilities. The inclusion of atomic polarizabilities following Thole's model allows also for the solvent molecules to be polarized. The QM/MM interactions are collected into an effective operator which is introduced directly into the Kohn-Sham equations. We will ignore the van der Waals interactions since we adopt supermolecular cluster obtained separately from a MD simulation and the structure is kept fixed during the QM/MM calculations. Therefore, the van der Waals contribution to the energy is a constant independent of the quantum part and can be obtained directly from the MD simulation.

As an initial application we will present dipole and quadrupole moments of water in aqueous solution with focus on choosing the atomic point charges, atomic polarizabilities, basis set and exchange-correlation (xc) potentials.

#### **II. THEORY**

In the QM/MM method the total (effective) Hamiltonian for the system is written as  $^{4-15}$ 

$$\hat{H} = \hat{H}_{\rm QM} + \hat{H}_{\rm QM/MM} + \hat{H}_{\rm MM}, \qquad (1)$$

where  $\hat{H}_{\rm QM}$  is the quantum mechanical Hamiltonian for the solute,  $\hat{H}_{\rm QM/MM}$  describes the interactions between solute and solvent, and  $\hat{H}_{\rm MM}$  describes the solvent–solvent interactions. In this work we focus on the description of the quantum part in the presence of a solvent. The solute–solvent interactions are therefore introduced into the vacuum Hamiltonian as an effective operator which are described in more details in the next section.

#### A. The discrete reaction field operator

The Discrete Reaction Field operator at a point  $r_i$  contains two terms

$$v^{\text{DRF}}(r_i) = v^{\text{el}}(r_i) + v^{\text{pol}}(r_i), \qquad (2)$$

where the first term,  $v^{el}$ , is the electrostatic operator and describes the Coulombic interaction between the QM system and the permanent charge distribution of the solvent molecules. The second term,  $v^{pol}$ , is the polarization operator and describes the many-body polarization of the solvent molecules, i.e., the change in the charge distribution of the solvent molecules due to interaction with the QM part and other solvent molecules. The charge distribution of the solvent is represented by atomic point charges, hence the electrostatic operator is given by

$$v^{\rm el}(r_i) = \sum_{s} \frac{q_s}{R_{si}} = \sum_{s} q_s T_{si}^{(0)}, \qquad (3)$$

where the zeroth order interaction tensor has been introduced and the index s runs over all atoms of the solvent molecules. In general the interaction tensor to a given order, n, can be written as

$$T_{pq,\alpha_1,\ldots,\alpha_n}^{(n)} = \nabla_{pq,\alpha_1} \ldots \nabla_{pq,\alpha_n} \left(\frac{1}{R_{pq}}\right), \tag{4}$$

where  $R_{pq}$  is the distance between the interacting entities.

The many-body polarization term is represented by induced atomic dipoles at the solvent molecules and the polarization operator is given by

$$\boldsymbol{v}^{\text{pol}}(\boldsymbol{r}_i) = \sum_{s} \mu_{s,\alpha}^{\text{ind}} \frac{R_{si,\alpha}}{R_{si}^3} = \sum_{s} \mu_{s,\alpha}^{\text{ind}} T_{si,\alpha}^{(1)}, \qquad (5)$$

where  $R_{si,\alpha}$  is a component of the distance vector and  $\mu_s^{\text{ind}}$  is the induced dipole at site *s*. For Greek indices the Einstein summation convention is employed. The induced dipoles are discussed in more detail in the next section.

#### B. The atomic induced dipoles

For a collection of atomic polarizabilities in an electric field, assuming linear response, the induced atomic dipole at site s is given by

$$\mu_{s,\alpha}^{\text{ind}} = \alpha_{s,\alpha\beta} \left( F_{s,\beta}^{\text{init}} + \sum_{t \neq s} T_{st,\beta\gamma}^{(2)} \mu_{t,\gamma}^{\text{ind}} \right), \tag{6}$$

where  $\alpha_{a,\alpha\beta}$  is a component of the atomic polarizability tensor at site *s*, which for an isotropic atom gives  $\alpha_{s,\alpha\beta} = \delta_{\alpha\beta}\alpha_s$ .  $F_{s,\beta}^{\text{init}}$  is the initial electric field at site *s* and the last term is the electric field from the other induced dipoles. The dipole interaction tensor,  $T_{st,\alpha\beta}^{(2)}$ , is given by

$$T_{st,\alpha\beta}^{(2)} = \frac{3R_{st,\alpha}R_{st,\beta}}{R_{st}^5} - \frac{\delta_{\alpha\beta}}{R_{st}^3}.$$
(7)

The initial field in Eq. (6) is given as a sum of three terms,

$$F_{t,\beta}^{\text{init}} = F_{t,\beta}^{\text{QM,el}} + F_{t,\beta}^{\text{QM,nuc}} + F_{t,\beta}^{\text{MM,q}}, \qquad (8)$$

where  $F_{t,\beta}^{\text{QM,el}}$  is the field arising from the electronic charge distribution of the QM part,

$$F_{t,\beta}^{\text{QM,el}} = -\int \rho(r_i) \frac{R_{it,\beta}}{R_{it}^3} dr_i = \int \rho(r_i) T_{it,\beta}^{(1)} dr_i$$
(9)

and  $F_{t,\beta}^{\text{QM,nuc}}$  is the field arising from the QM nuclei,

$$F_{t,\beta}^{\text{QM,nuc}} = \sum_{m} \frac{Z_{m} R_{mt,\beta}}{R_{mt}^{3}} = -\sum_{m} Z_{m} T_{mt,\beta}^{(1)}$$
(10)

and  $F_{t,\beta}^{MM,q}$  is the field arising from the point charges at the solvent molecules,

$$F_{t,\beta}^{\mathrm{MM},q} = \sum_{s} ' \frac{q_{s} R_{st,\beta}}{R_{st}^{3}} = -\sum_{s} ' q_{s} T_{st,\beta}^{(1)}.$$
(11)

The prime in Eq. (11) indicates that the sum is restricted to sites which do not belong to the same molecule. Since the induced dipole in Eq. (6) depends on the induced dipoles at the other sites these equations have to be solved self-consistently. This can be done analytically by rewriting the equations into a  $3N \times 3N$  linear matrix equation, with *N* the number of atoms, as

$$A\mu^{\rm ind} = F^{\rm init} \tag{12}$$

and the components of the matrix,  $A_{st,\alpha\beta}$ , given by

$$A_{st,\alpha\beta} = (\alpha_{s,\alpha\beta}^{-1} \delta_{st} - T_{st,\alpha\beta}^{(2)}).$$
<sup>(13)</sup>

This matrix equation can then be solved for the induced dipoles using standard mathematical tools for solving linear equations. The inverse of the matrix *A*, the so called relay matrix, is a generalized polarizability matrix which describes the total linear response of the discrete solvent molecules.

#### C. Damping of the induced dipoles

3.7

If  $F^{\text{init}}$  is an uniform external field the polarizability of the classical system can be written as<sup>41</sup>

$$\alpha_{\alpha\beta}^{\text{mol}} = \sum_{p,q}^{N} B_{pq,\alpha\beta}, \qquad (14)$$

where  $\mathbf{B}$  is the relay matrix defined in a supermatrix notation as

$$\mathbf{B} = \mathbf{A}^{-1} = (\boldsymbol{\alpha}^{-1} - \mathbf{T}^{(2)})^{-1}.$$
 (15)

The polarizability parallel,  $\alpha_{\parallel}$ , and perpendicular,  $\alpha_{\perp}$ , to the axes connecting two interacting atoms, *p* and *q*, are given by Silberstein's equations,<sup>42</sup> which are the exact solutions to Eq. (14),

$$\alpha_{\parallel} = \frac{\alpha_p + \alpha_q + 4\,\alpha_p\,\alpha_q/r^3}{1 - 4\,\alpha_p\,\alpha_q/r^6},\tag{16}$$

$$\alpha_{\perp} = \frac{\alpha_p + \alpha_q - 2\alpha_p \alpha_q / r^3}{1 - \alpha_p \alpha_q / r^6}.$$
(17)

From Eqs. (16) and (17) it is seen that when *r* approaches  $(4 \alpha_p \alpha_q)^{1/6}$ ,  $\alpha_{\parallel}$  goes to infinity and becomes negative for even shorter distances. In order to avoid this "polarizability catastrophe" Thole<sup>43</sup> modified the dipole interaction tensor using smeared-out dipoles. The dipole interaction tensor was first rewritten in terms of a reduced distance  $u_{pq,\beta} = R_{pa,\beta}/(\alpha_p \alpha_q)^{1/6}$  as

$$T_{pq,\beta\gamma}^{(2)} = (\alpha_p \alpha_q)^{1/2} t(u_{pq}) = (\alpha_p \alpha_q)^{1/2} \frac{\partial^2 \phi(u_{pq})}{\partial u_{pq,\beta} \partial u_{pq,\gamma}},$$
(18)

where  $\phi(u_{pq})$  is a spherically symmetric potential of some model charge distribution  $\rho$ . The screened dipole interaction tensor can be written as

$$T_{pq,\alpha\beta}^{(2)} = \frac{3f_{pq}^{T}R_{pq,\alpha}R_{pq,\beta}}{R_{pq}^{5}} - \frac{f_{pq}^{E}\delta_{\alpha\beta}}{R_{pq}^{3}},$$
(19)

where the damping functions  $f_{pq}^T$  and  $f_{pq}^E$  have been introduced. If we consider a exponential decaying charge distribution the screening functions in Eq. (19) are given by<sup>44</sup>

$$f_{pg}^{E} = 1 - [1 + s_{pq} + \frac{1}{2}s_{pq}^{2}]\exp(-s_{pq})$$

and

$$f_{pg}^{T} = f_{pg}^{E} - \frac{1}{6}s_{pq}^{3} \exp(-s_{pq}), \qquad (20)$$

where the term  $s_{pq}$  is give by  $s_{pq} = aR_{pq}/(\alpha_p \alpha_q)^{1/6}$ , with *a* the screening length, and  $\alpha_p$  the atomic polarizability of atom *p*.

#### D. The QM/MM interaction energy

The QM/MM interaction energy is given by a sum of three terms,

$$E^{\text{QM/MM}} = E^{\text{elst,el}} + E^{\text{elst,nuc}} + E^{\text{ind}}, \qquad (21)$$

where the first two terms are the electrostatic interaction between the QM electrons and the classical point charges

$$E^{\text{elst,el}} = -\sum_{s} q_{s} \int \rho(r_{i}) \frac{1}{R_{is}} dr_{i}$$
(22)

and the electrostatic interaction between the QM nuclei and the point charges

$$E^{\text{elst,nuc}} = \sum_{s} q_{s} \sum_{m} \frac{Z_{m}}{R_{ms}},$$
(23)

respectively.

The last term is the induction energy and is given by  $^{26,46}$ 

$$E^{\text{ind}} = -\frac{1}{2}\mu^{\text{ind}}F^{\text{QM}},\tag{24}$$

where  $F^{QM}$  is the electric field arising from the QM system, i.e., the field from the QM electrons and nuclei. The induction energy consist of the sum of the energy of the induced dipoles in the electric field and the polarization cost, i.e., the energy needed for creating the induced dipoles.

#### E. The effective Kohn–Sham equations

The effective Kohn–Sham (KS) equations which has to be solved for the combined QM/MM system is given by

$$h_{\rm KS}\phi_i(r) = \epsilon_i\phi_i(r),\tag{25}$$

where  $h_{\rm KS}$  is the effective KS-operator and  $\phi_i$  is the KS orbital with energy  $\epsilon_i$ . The effective KS-operator consists of the sum of the vacuum operator,  $h_{\rm KS}^0$ , and the reaction field operator,  $v^{\rm DRF}$ , with the vacuum KS-operator given as

$$h_{\rm KS}^0 = -\frac{1}{2}\nabla^2 + V_N(r) + V_C(r) + v_{\rm XC}(r)$$
(26)

$$= -\frac{1}{2}\nabla^2 - \sum_{m} \frac{Z_m}{|r-R_m|} + \int \frac{\rho(r)}{|r-r'|} dr' + \frac{\delta E_{\rm XC}}{\delta\rho(r)},$$
(27)

where the individual terms in the vacuum operator are the kinetic operator, the nuclear potential, the Coulomb potential (or Hartree potential), and the xc-potential, respectively. The DRF model has been implemented into a local version of the AMSTERDAM DENSITY FUNCTIONAL (ADF) program package.<sup>47,48</sup> In the ADF the KS equations are solved by numerical integration which means that the effective KS-operator has to be evaluated in each integration point. Since the numerical integration grid is chosen on the basis of the quantum part alone care must be taken when evaluating the DRF operator if the integration points are close to a classical atom. In order to avoid numerical instabilities we introduce a damping of the operator at small distances which is modeled by modifying the distance  $R_{ij}$  to obtain a scaled distance  $S_{ij}$ ,<sup>49</sup>

$$S_{ii} = v_{ii}R_{ii} = f(R_{ii}),$$
 (28)

where  $v_{ij}$  is a scaling factor and  $f(R_{ij})$  an appropriately chosen function of  $R_{ij}$ . Furthermore, each component of  $R_{ij}$  is also scaled by  $v_{ij}$ , so the reduced distance becomes,

$$S_{ij} = \sqrt{S_{ij,\alpha}} S_{ij,\alpha} = v_{ij} \sqrt{R_{ij,\alpha}} = v_{ij} R_{ij,\alpha}, \qquad (29)$$

consistent with the definition in Eq. (28). The damped operator can thus be obtained by modifying the interaction tensors in Eqs. (3) and (5),

$$T_{ij,\alpha_1,\ldots,\alpha_n}^{(n)} = \nabla_{\alpha_1} \cdots \nabla_{\alpha_n} \left(\frac{1}{S_{ij}}\right), \tag{30}$$

which is equivalent to replacing  $R_{ij}$  by  $S_{ij}$  and  $R_{ij,\alpha}$  by  $S_{ij,\alpha}$  in the regular formulas for the interaction tensors. The particular form of the scaling function employed here is<sup>49</sup>

$$f(r_{pq}) = \frac{r_{pq}}{\operatorname{erf}(r_{pq})},\tag{31}$$

which was obtained by considering the interaction between two Gaussian charge distributions with unity exponents.

#### **III. COMPUTATIONAL DETAILS**

All calculations have been performed with the ADF program package. The calculations of the polarizability of water in the gas phase have been done using time-dependent DFT as implemented in the RESPONSE code<sup>50-52</sup> in the ADF. The ADF program uses basis sets of Slater functions where in this work a triple zeta valence plus polarization (in ADF basis set V), here denoted TZ2P, is chosen as the basis. The basis set is then augmented with diffuse functions giving TZ2P+,<sup>51</sup> added s,p, and d functions or TZ2P+++,<sup>53</sup> added two s,p,d, and f functions. The TZ2P+++ basis set is expected to give results close to basis set limit the for (hyper-)polarizabilities.53

We also tested different xc potentials, the Local Density Approximation (LDA), Becke-Lee-Yang-Parr (BLYP),54,55 the Becke–Perdew (BP),<sup>54,56</sup> and the van Leeuwen– Baerends (LB94) (Ref. 57) potentials. The BLYP and BP are examples of typical Generalized Gradient Approximations (GGAs) potentials, whereas the LB94 is an example of a so-called asymptotic correct potential due to the correct Coulombic decay of the potential at large distances. The water structure we use in this work was taken from Ref. 39 and consists of 128 rigid water molecule where one molecule, the solute, is treated quantum mechanically. The total structure was obtained from a MD simulation using a polarizable force field<sup>27</sup> and the details about the simulation can be found in Ref. 58. The intra molecular geometry of the water molecules was that in gas phase, i.e.,  $R_{O-H}=0.9572$  Å and  $\angle_{HOH}$ =104.49°. The solute water molecule was placed in the xz-plane with the z-axis bisecting the H–O–H angle. Results obtained using this structure will be references as "liquid" phase results. We will perform one QM/MM calculation and therefore the molecular properties will not be averaged over different solvent configurations. However, the choice of this particular water structure allows for a direct comparison with results obtained from a similar model within a (multiconfigurational) Self-Consistent-Field/Molecular Mechanics (MC-SCF/MM) (Ref. 59) or a Coupled Cluster/Molecular Mechanics (CC/MM) (Ref. 58) approach. Therefore, it is possible to make a detailed comparison between wave function methods and the DFT method for liquid phase calculations.

#### **IV. RESULTS**

#### A. Solvent models

We investigated six different models for representing the solvent molecules using atomic parameters in three nonpolarizable and three polarizable models. The atomic parameters used in the different models are given in Table I along with the molecular dipole moment and polarizability which they reproduce. The first two nonpolarizable models, i.e., charge only models, where obtained by using different ways of partitioning the electronic charge distribution into atomic charges. The first charge model, MUL, is obtained using the Mulliken population analysis and the second charge model,

TABLE I. Atomic parameters for the different solvent models in atomic units and the molecular dipole moment,  $\mu$ , mean polarizability,  $\bar{\alpha}$ , and polarizability anisotropy,  $\Delta \alpha$ , modeled by the atomic parameters. Dipole moment in Debye and mean polarizability and polarizability anisotropy in atomic units. The mean polarizability is defined as  $\bar{\alpha} = (\alpha_{xx} + \alpha_{yy} + \alpha_{zz})/3$  and the polarizability anisotropy as  $\Delta \alpha = (1/2)^{1/2} [(\alpha_{xx} - \alpha_{yy})^2 + (\alpha_{xx} - \alpha_{zz})^2 + (\alpha_{zz} - \alpha_{yy})^2]^{1/2}$ .

Model	$q_{\rm H}$	$q_{0}$	$\alpha_{ m H}$	$\alpha_0$	$\mu$	$\bar{\alpha}$	$\Delta \alpha$
MUL	0.3040	-0.6080	0	0	1.71	0	0
VDD	0.1370	-0.2740	0	0	0.77	0	0
SPC	0.3345	-0.6690	0	0	1.88	0	0
Thole-S	0.3345	-0.6690	2.7929	5.7494	1.88	10.06	4.32
Thole-I	0.3345	- 0.6690	0	9.7180	1.88	9.72	0
Thole-A	0.3345	-0.6690	0.0690	9.3005	1.88	9.62	0.51

TABLE II. Dipole and quadrupole moments of water in the gas phase and in the "liquid phase" and the induced dipole moment,  $\Delta \mu$  in going from the gas phase to the "liquid phase" using different charge and polarization models. Dipole and induced dipole moments in Debye and quadrupole moment in atomic units. All calculations have been made with LDA and the TZ2P basis set.

Model	$\mu$	$\Delta \mu$	$Q_{xx}$	$Q_{yy}$	$Q_{zz}$
Vacuum	1.86		1.83	-1.91	0.08
Without polarization					
MUL	2.34	0.48	1.97	-2.09	0.12
VDD	2.08	0.22	1.90	-1.99	0.10
SPC	2.39	0.53	1.98	-2.10	0.12
With polarization					
Thole-S	2.69	0.83	2.05	-2.16	0.11
Thole-I/Thole-A	2.58	0.72	2.04	-2.17	0.13

VDD, using the so-called Voronoi deformation density method, for a descriptions of the partitioning schemes, see Ref. 47. The last charge model, SPC, is adopted from Ref. 27 and is identical to the charge model used in the reference works of Refs. 58 and 59. The point charges in model SPC have been chosen to reproduce the experimental gas phase dipole moment of 1.85 D for the SPC water geometry,<sup>27</sup> however, since we use a different geometry for water the dipole moment will be slightly larger here. The atomic polarizabilities used in the three polarizable solvent models were all obtained using Thole's model, i.e., Eq. (14), for reproducing the molecular polarizability. The screening parameter, a = 2.1304, used in all three models was taken from Ref. 44. The screening parameter together with atomic model polarizability parameters were obtained by fitting to the experimental mean polarizability of 52 molecules. The model using these atomic polarizability parameters will be denoted Thole-S(tandard). In the second model, Thole-I(sotropic), the atomic polarizability parameters where chosen to reproduce the isotropic mean polarizability of 9.718 a.u. used in the reference works.<sup>58,59</sup> In the third model, Thole-A(nisotropic), the atomic polarizability was chosen so as to reproduce the full molecular polarizability tensor of water calculated using CCSD(T) which was taken from Ref. 60. The results for the dipole and quadrupole moments for water in the gas phase and in the "liquid" phase and also the induced dipole moment,  $\Delta \mu$ , in going from the gas phase to the "liquid" phase using the six different solvent models are presented in Table II. We only present results for the diagonal components of the quadrupole moment although off-diagonal elements are present due to the structure of the water cluster. However, these off-diagonal elements will become zero when averaged over more water configurations. The results using the nonpolarizable solvent models shows that a 10% change in the atomic parameters, the difference between MUL and SPC, also gives a 10% change in the induced dipole moment. Especially, the VVD charges underestimate the induced dipole moment and illustrates the problem using only point charges without including higher order moments in some way. Therefore, it is important to chose the atomic charges so that they give a good dipole moment and maybe even reasonable higher order moments. However, for water it is not possible to accurately reproduce both dipole moment and higher order

moments using only atomic point charges. We will therefore adopt the SPC model as starting point for the polarizable models. From the results in Table II it is seen that including the polarization of the solvent molecules increases the dipole moment and quadrupole moment of the "liquid phase" and therefore it is very important to include this polarization, especially for the dipole moment. This has also been found in previous studies using wave function methods.35,58 Comparing the three different polarization models we see that there is no difference between Thole-I and Thole-A. Therefore, for water, the effect of distributing the polarizability into atomic contributions is negligible due to the small polarizability anisotropy of the water molecule. In general it is expected that a distributed polarizability approach will give better results than an approach using only a (anisotropic) polarizability located at a single site, especially as the size of the solvent molecule increases.<sup>61</sup> However, as seen from the differences in the results using Thole-S and Thole-A it is important when using distributed polarizability that also the anisotropy is accounted for correctly. In the rest of our work we will use the Thole-A solvent model since it is found that the differences between this solvent model and the one used in the reference work is negligible.

#### B. Basis sets

In Table III we present results for the dipole moment and

TABLE III. Dipole moment, quadrupole moment, and mean polarizability for water in the gas phase and dipole moment, induced dipole moment and quadrupole moment for water in "liquid phase" using the Thole-A solvent model and different basis sets. Dipole and induced dipole moment in Debye. Quadrupole moment and mean polarizability in atomic units.

Basis set	$\mu$	$\Delta \mu$	$Q_{xx}$	$Q_{yy}$	$Q_{zz}$	$\bar{\alpha}$
Gas phase						
TZ2P	1.86		1.84	-1.91	0.08	8.50
TZ2P+	1.87		1.83	-1.90	0.07	10.47
TZ2P+++	1.86		1.84	-1.91	0.07	10.55
"Liquid" phase						
TZ2P	2.58	0.72	2.04	-2.17	0.13	
TZ2P+	2.68	0.81	2.07	-2.17	0.10	
TZ2P+++	2.69	0.83	2.08	-2.19	0.11	

TABLE IV. Dipole moment, quadrupole moment, and mean polarizability for water in the gas phase and dipole moment, induced dipole moment and quadrupole moment for water in "liquid phase" using the Thole-A solvent model, TZ2P+, and different xc-potentials. Dipole and induced dipole moment in Debye. Quadrupole moment and mean polarizability in atomic units.

Method	$\mu$	$\Delta \mu$	$Q_{xx}$	$Q_{yy}$	$Q_{zz}$	$\bar{\alpha}$
Gas phase						
LDA	1.87		1.83	-1.90	0.07	10.47
BLYP	1.81		1.79	-1.85	0.06	10.82
BP	1.81		1.80	-1.86	0.06	10.20
LB94	1.97		1.72	-1.81	0.09	9.14
CCSD <sup>a</sup>	1.85		1.82	-1.90	0.08	
"Liquid" phase						
LDA	2.68	0.81	2.07	-2.17	0.10	
BLYP	2.63	0.82	2.04	-2.13	0.09	
BP	2.63	0.82	2.04	-2.13	0.09	
LB94	2.65	0.68	1.93	-2.04	0.11	
CCSD/MM <sup>a</sup>	2.71	0.86	2.08	-2.16	0.08	

<sup>a</sup>Results using a aug-cc-pVTZ basis set taken from Ref. 58.

quadrupole moment both in the gas phase and in the "liquid" phase using the TZ2P, TZ2P+, and TZ2P+++ basis sets. The static mean polarizability in the gas phase is also shown. In the gas phase the dipole moment and quadrupole moment is converged already using the TZ2P basis set. For the polarizability the inclusion of extra diffuse functions are needed in order to achieve accurate results. We see that the inclusion of the first order field induced polarization (FIP) functions of Zeiss *et al.*<sup>62</sup> in basis set TZ2P+ gives a mean polarizability in good agreement with the result using the very large basis set TZ2P+++.

In the "liquid" phase the dipole moment is increased considerably by including diffuse functions in the basis set, whereas the basis set effects on the quadrupole moment are negligible. The  $\Delta \mu$  is increased by 12.5% using TZ2P+ and by 15% using TZ2P+++ compared with the TZ2P basis set. The changes in the  $\Delta \mu$  with the basis sets are in good agreement with the changes in the gas phase polarizability. Therefore, for calculating the dipole moment in the liquid phase the inclusion of additional diffuse basis functions, normally associated with calculations of the gas phase polarizability, are required for obtaining good results. This has also been observed in a previous study<sup>63</sup> using a mean field QM/MM approach at the Hartree–Fock level of theory.

#### C. xc-potentials

Table IV shows the dipole moment, quadrupole moment, and mean polarizability of water in the gas phase and dipole moment, induced dipole moment and quadrupole moment in the "liquid" phase calculated using different xc-potentials. The results are compared with results obtained for the same water structure using a aug-cc-pVTZ basis set and a CCSD/MM (Ref. 58) approach. In the gas phase the two GGA potentials, BLYP and BP, give identical results for dipole and quadrupole moments and compared with LDA slightly lower values. There is very good agreement between the LDA results and the CCSD results for both dipole and quadrupole moments. For a series of small molecules it has

TABLE V. Comparison of continuum and discrete models for the prediction of the dipole and quadrupole moments of water in the liquid phase. Dipole and induced dipole moments in Debye. Quadrupole moment in atomic units.

Method	μ	$\Delta \mu$	$Q_{xx}$	$Q_{yy}$	$Q_{zz}$
Continuum model					
LDA/COSMO <sup>a</sup>	2.26	0.39	1.92	-2.04	0.13
CCSD/D.C. <sup>b</sup>	2.19	0.34	1.91	-2.09	0.13
Discrete model					
LDA/DRF	2.68	0.81	2.07	-2.17	0.10
HF/MM <sup>c</sup>	2.77	0.79	2.19	-2.01	-0.18
CCSD/MM <sup>c</sup>	2.71	0.86	2.08	-2.16	0.08

<sup>a</sup>Dielectric constant  $\epsilon$ =78.8 and  $R_{\rm H}$ =1.44 Å and  $R_{\rm O}$ =1.80 Å.

<sup>b</sup>Dielectric continuum model using a aug-cc-pVTZ basis set taken from Ref. 58.

<sup>c</sup>Results using a aug-cc-pVTZ basis set taken from Ref. 58.

been shown that LDA predicts good dipole and quadrupole moments compared with experimental results, especially for the water molecule.<sup>64,65</sup> The use of an asymptotic correct functional, LB94, increases the dipole moment and lowers the quadrupole moment compared with LDA and made the agreement with the CCSD results less good. For the mean polarizability BLYP gives a larger value, 10.82 a.u., and BP a smaller value, 10.20 a.u., compared with the LDA results of 10.47 a.u. but all values are still larger than the CCSD(T)results of 9.62 a.u. The LB94 results of 9.14 a.u. is much lower than the LDA results and in better agreement with the CCSD(T) result. The shifts in the dipole and quadrupole moment in going from the gas phase to the "liquid" phase predicted using LDA or one of the GGA potentials are almost identical. The "liquid" phase dipole and quadrupole moments predicted with the GGA's are slightly lower than the LDA results and the differences are identical with the differences found in the gas phase. The solvent shifts for dipole and quadrupole moments predicted with LB94 are smaller than the shifts found using LDA, in agreement with the smaller gas phase polarizability found with LB94 compared with LDA. The "liquid" phase dipole moment found with LB94 compares well with the LDA value but the quadrupole moment is smaller. Also in the "liquid" phase there is a very good agreement between the LDA results and the CCSD/MM results. Since the induced dipole moment correlates well with the gas phase polarizability it indicates that to get a good description of the dipole moment in the liquid phase the gas phase dipole moment and polarizability must also be properly described.

# D. Comparison of theoretical predictions for dipole and quadrupole moments in liquid phase

A comparison between some continuum and discrete models for calculating the dipole and quadrupole moments of "liquid" water is presented in Table V. The continuum models are the CCSD/D.C. model (Ref. 58) and the LDA/COSMO model<sup>66</sup> and the discrete models are the CCSD/MM and HF/MM models from Ref. 58 and the LDA/DRF model from this work. In all models the same geometry of the water molecules is used and in all discrete models also the same solvent structure is used. From the results in Table V we see that using a continuum model the dipole and quadrupole mo-

ments of the liquid phase are underestimated compared with the discrete models. The induced dipole moment predicted with the continuum models are a factor of 2 smaller than the results from the continuum model. The agreement between the LDA results and the CCSD results are very good both using the continuum model and the discrete model. Compared with the HF/MM results we find that the LDA/DRF results are in much better agreement with the CCSD/MM results.

There has been put a lot of effort into predicting the average dipole moment of liquid water since there is no way of determining this directly from experiment, although a recent experimental study<sup>67</sup> of liquid water using neutron diffraction predicts a dipole moment of  $2.9\pm0.6$  D. The average dipole moment of liquid water estimated using the experimental static dielectric constant is about 2.6 D.<sup>68,69</sup> The most commonly accepted value for the dipole moment of liquid water is 2.6 D (Ref. 70) arising from an induction model study on ice Ih. However, this study has been repeated recently using more accurate input parameters giving an average dipole moment of 3.1 D.<sup>71</sup> The latter value is in good agreement with an ab initio MD simulation of liquid water using maximally localized Wannier functions for describing the molecular charge distribution.<sup>72,73</sup> A different *ab initio* MD simulation of liquid water where the molecular charge distribution is defined using Bader's zero flux surface gives a smaller average dipole moment of 2.5 D.<sup>22</sup> They also reported results for the average dipole moment of ice Ih and found that it is considerably larger than the liquid phase results. The dependency of the molecular results on the partitioning of the charge distribution was clearly shown in a first principle study on ice Ih,<sup>20</sup> where the average dipole moment varied between 2.3 and 3.1 D dependent on the partitioning scheme. This study also showed that the dipole moment obtained using Bader's zero flux surface was smaller than the results predicted with the accurate induction model. To summarize, we believe that the dipole moment of liquid water is smaller than found in ice Ih, therefore 3.1 D is most likely an upper limit. Furthermore, since Bader's zero flux surface underestimates the dipole moment in ice Ih, 2.5 D is probably a lower limit for the average dipole moment in liquid water. Our result for the dipole moment of liquid water of 2.68 D is in good agreement with previously reported studies<sup>35,58,59,74-76</sup> and also within the above suggested limits.

## **V. CONCLUSIONS**

In this work we have presented theory and implementation of a discrete reaction field model within density functional theory. The model combines a quantum mechanical description at the DFT level of theory of the solute and a classical description of the discrete solvent molecules. The solvent molecules are described using atomic point charges for representing the permanent electronic charge distribution and atomic polarizabilities for describing the solvent polarization arising from many-body interactions. All atomic parameters have been chosen to reproduce molecular gas phase properties, i.e., the atomic charges reproduces the molecular gas phase dipole moment and the atomic polarizabilities reproduce the molecular gas phase polarizability tensor using Thole's model for distributed polarizabilities. The model was tested using a water cluster of 128 water molecules taken from a previous study using a similar solvent model but the solute molecule was treated either at the HF or CCSD level of theory, thereby making it possible to assess the quality of DFT for calculating molecular properties of liquids. The results show that the inclusion of the polarization of the solvent molecules is essential for an accurate prediction of liquid phase properties. Also, surprisingly, a very good agreement was found between the LDA results and the CCSD results for both the dipole and quadrupole moments in the liquid phase. The use of a GGA xc-potential only affected the results slightly whereas using an asymptotic correct functional affected the result more strongly and made the agreement with the CCSD results less well. It was found that the induced dipole moment correlates well with the gas phase molecular polarizability indicating that a good xc-potential must provide both good gas phase dipole moment and molecular polarizability in order to accurately describe the molecular properties in the liquid phase. The results for the dipole moment of 2.68 D are in good agreement with previous theoretical predictions and also with results based on experimental predictions.

### ACKNOWLEDGMENTS

One of the authors (L.J.) gratefully acknowledges The Danish Research Training Council for financial support. The authors are grateful to Jacob Kongsted, Anders Osted, and Dr. Kurt V. Mikkelsen for supplying the water cluster configuration and a preprint of Ref. 58.

- <sup>1</sup>J. Tomasi and M. Persico Chem. Rev. 94, 2027 (1994).
- <sup>2</sup>C. J. Cramer and D. G. Truhlar, Chem. Rev. 99, 2161 (1999).
- <sup>3</sup>M. Orozco and F. J. Luque, Chem. Rev. **100**, 4187 (2000).
- <sup>4</sup>A. Warshel and M. Levitt, J. Mol. Biol. 103, 227 (1976).
- <sup>5</sup>B. T. Thole and P. Th. van Duijnen. Theor. Chim. Acta 55, 307 (1980).
- <sup>6</sup>U. C. Singh and P. A. Kollman, J. Comput. Chem. 7, 718 (1986).
- <sup>7</sup>P. A. Bash, M. J. Field, and M. Karplus, J. Am. Chem. Soc. **109**, 8092 (1987).
- <sup>8</sup>M. J. Field, P. A. Bash, and M. Karplus, J. Comput. Chem., **11**, 700 (1990).
- <sup>9</sup>V. Luzhkov and A. Warshel, J. Comput. Chem. 13, 199 (1992).
- <sup>10</sup> R. V. Stanton, D. S. Hartsough, and K. M. Merz, J. Phys. Chem. **97**, 11868 (1993).
- <sup>11</sup>A. H. de Vries, P. Th van Duijnen, A. H. Juffer, J. A. C. Rullmann, J. P. Dijkman, H. Merenga, and B. T. Thole, J. Comput. Chem. **16**, 37 (1995).
- <sup>12</sup> I. Tuñón, M. T. C. Martins-Costa, C. Millot, M. F. Ruiz-López, and J. L. Rivail, J. Comput. Chem. **17**, 19 (1996).
- <sup>13</sup>J. Gao, "Methods and applications of combined quantum mechanical and molecular mechanical potentials," in *Reviews in Computational Chemistry*, edited by K. B. Lipkowitz and D. B. Boyd (VCH, New York, 1995), Vol. 7, pp. 119–185.
- <sup>14</sup>J. Gao, Acc. Chem. Res. **29**, 298 (1996).
- <sup>15</sup> Combined Quantum Mechanical and Molecular Mechanical Methods, edited by J. Gao and M. A. Thompson, ACS Symposium Series (American Chemical Society, Washington, D.C., 1998), Vol. 712.
- <sup>16</sup> V. Barone, M. Cossi, and T. Tomasi, J. Chem. Phys. **107**, 3210 (1997).
- <sup>17</sup>A. Pullman and B. Pullman, Q. Rev. Biophys. 7, 505 (1975).
- <sup>18</sup>T. Wesolowski and A. Warshel, J. Phys. Chem. 98, 5183 (1994).
- <sup>19</sup>R. Car and M. Parrinello, Phys. Rev. Lett. **55**, 2471 (1985).
- <sup>20</sup>E. R. Batista, S. S. Xantheas, and H. Jónsson, J. Chem. Phys. **111**, 6011 (1999).
- <sup>21</sup>L. Jensen, M. Swart, P. Th. van Duijnen, and J. G. Snijders, J. Chem. Phys. **117**, 3316 (2002).

- <sup>22</sup>L. Delle Site, A. Alavi, and R. M. Lynden-Bell, Mol. Phys. **96**, 1683 (1999).
- <sup>23</sup>O. Engkvist, P.-O. Åstrand, and G. Karlström, Chem. Rev. **100**, 4087 (2000).
- <sup>24</sup> Y. Tu and A. Laaksone, J. Chem. Phys. **111**, 7519 (1999).
- <sup>25</sup>M. Freindorf and J. Gao, J. Comput. Chem. **17**, 386 (1996).
- <sup>26</sup>J. A. C. Rullmann and P. Th. van Duijnen, Mol. Phys. **63**, 451 (1988).
   <sup>27</sup>P. Ahlström, A. Wallqvist, S. Engström, and B. Jönsson, Mol. Phys. **68**, 563 (1989).
- <sup>28</sup>S. Kuwajima and A. Warshel, J. Phys. Chem. **94**, 460 (1990).
- <sup>29</sup>L. X. Dang, J. Chem. Phys. 97, 2183 (1992).
- <sup>30</sup>J.-C. Soetens and C. Milot, Chem. Phys. Lett. 235, 22 (1995).
- <sup>31</sup>L. X. Dang and T.-M. Chang, J. Chem. Phys. **106**, 8149 (1997).
- <sup>32</sup>C. J. Burnham, J. Li, S. S. Xantheas, and M. Leslie, J. Chem. Phys. **110**, 4566 (1999).
- <sup>33</sup> T. A. Halgren and W. Damm, Curr. Opin. Struct. Biol. **11**, 236 (2001).
- <sup>34</sup>M. A. Thompson and G. K. Schenter, J. Phys. Chem. 99, 6374 (1995).
- <sup>35</sup>G. Jansen, F. Colonna, and J. G. Ángyán, Int. J. Quantum Chem. 58, 251 (1996).
- <sup>36</sup> P. N. Day, J. H. Jensen, M. S. Gordon, S. P. Webb, W. J. Stevens, M. Krauss, D. Garmer, H. Basch, and D. Cohen, J. Chem. Phys. **105**, 1968 (1996).
- <sup>37</sup>J. Gao and M. Freindorf, J. Phys. Chem. A **101**, 3182 (1997).
- <sup>38</sup>J. Gao, J. Comput. Chem. **18**, 1061 (1997).
- <sup>39</sup>T. D. Poulsen, J. Kongsted, A. Osted, P. R. Ogilby, and K. V. Mikkelsen, J. Chem. Phys. **115**, 2393 (2001).
- <sup>40</sup> M. Dupuis, M. Aida, Y. Kawashima, and K. Hirao, J. Chem. Phys. **117**, 1242 (2002).
- <sup>41</sup>J. Applequist, J. R. Carl, and K. F. Fung, J. Am. Chem. Soc. **94**, 2952 (1972).
- <sup>42</sup>L. Silberstein, Philos. Mag. **33**, 521 (1917).
- <sup>43</sup>B. T. Thole, Chem. Phys. **59**, 341 (1981).
- <sup>44</sup>P. Th. van Duijnen and M. Swart, J. Phys. Chem. A 102, 2399 (1998).
- <sup>45</sup>L. Jensen, P.-O. Åstrand, K. O. Sylvester-Hvid, and K. V. Mikkelsen, J. Phys. Chem. A **104**, 1563 (2000).
- <sup>46</sup>C. J. F. Böttcher, *Theory of Electric Polarization*, 2nd ed. (Elsevier, Amsterdam, 1973), Vol. 1.
- <sup>47</sup>G. te Velde, F. M. Bickelhaupt, E. J. Baerends, C. Fonseca Guerra, S. J. A. van Gisbergen, J. G. Snijders, and T. Ziegler, J. Comput. Chem. **22**, 931 (2001).
- <sup>48</sup> ADF 2000.01. http://www.scm.com, 2000.
- <sup>49</sup>L. Jensen, P.-O. Astrand, A. Osted, J. Kongsted, and K. V. Mikkelsen, J. Chem. Phys. **116**, 4001 (2002).

- <sup>50</sup> S. J. A. van Gisbergen, J. G. Snijders, and E. J. Baerends, Comput. Phys. Commun. **118**, 119 (1999).
- <sup>51</sup>S. J. A. van Gisbergen, J. G. Snijders, and E. J. Baerends, J. Chem. Phys. **103**, 9347 (1995).
- <sup>52</sup>S. J. A. van Gisbergen, J. G. Snijders, and E. J. Baerends, J. Chem. Phys. 109, 10644 (1998).
- <sup>53</sup>S. J. A. van Gisbergen, J. G. Snijders, and E. J. Baerends, J. Chem. Phys. 109, 10657 (1998).
- <sup>54</sup>A. D. Becke, Phys. Rev. A **38**, 3098 (1988).
- <sup>55</sup>C. L. Lee, W. Yang, and R. G. Parr, Phys. Rev. B 37, 785 (1988).
- <sup>56</sup>J. P. Perdew, Phys. Rev. B **33**, 8822 (1986).
- <sup>57</sup> R. van Leeuwen and E. J. Baerends, Phys. Rev. A 49, 2421 (1994).
- <sup>58</sup> J. Kongsted, A. Osted, K. V. Mikkelsen, and O. Christiansen, Chem. Phys. Lett. **363**, 379 (2002).
- <sup>59</sup>T. D. Poulsen, P. R. Ogilby, and K. V. Mikkelsen, J. Chem. Phys. **116**, 3730 (2002).
- <sup>60</sup>G. Maroulis, Chem. Phys. Lett. 289, 403 (1998).
- <sup>61</sup>F. C. Grozemar, R. W. J. Zijlstra, and P. Th. van Duijnen, Chem. Phys. 256, 217 (1999).
- <sup>62</sup>G. D. Zeiss, W. R. Scott, N. Suzuki, and D. P. Chong, Mol. Phys. **37**, 1543 (1979).
- <sup>63</sup> M. L. Sanchez Mendoza, M. A. Aguilar, and F. J. Olivares del Vall, J. Mol. Struct.: THEOCHEM 426, 181 (1998).
- <sup>64</sup> P. Duffy, D. P. Chong, and M. Dupuis, J. Chem. Phys. 102, 3312 (1995).
- <sup>65</sup>F. De Proft, F. Tielens, and P. Geerlings, J. Mol. Struct.: THEOCHEM 506, 1 (2000).
- <sup>66</sup>C. C. Pye and T. Ziegler, Theor. Chim. Acta 101, 396 (1999).
- <sup>67</sup> Y. S. Badyal, M.-L. Saboungi, D. L. Price, S. D. Shastri, D. R. Haeffner, and A. K. Soper, J. Chem. Phys. **112**, 9206 (2000).
- <sup>68</sup>S. L. Carnie and G. N. Patey, Mol. Phys. 47, 1129 (1982).
- <sup>69</sup> K. Watanabe and M. L. Klein, Chem. Phys. 131, 157 (1989).
- <sup>70</sup>C. Coulson and D. Eisenberg, Proc. R. Soc. London, Ser. A **291**, 445 (1966).
- <sup>71</sup> E. R. Batisa, S. S. Xantheas, and H. Jónsson, J. Chem. Phys. **109**, 4546 (1998).
- $^{72}\mbox{P}.$  L. Silverstrelli and M. Parrinello, Phys. Rev. Lett. 82, 3308 (1999).
- <sup>73</sup>P. L. Silverstrelli and M. Parrinello, J. Chem. Phys. 111, 3572 (1999).
- <sup>74</sup>L. X. Dang, J. Phys. Chem. B **192**, 620 (1998).
- <sup>75</sup>A. V. Gubskaya and P. G. Kusalik, Mol. Phys. 99, 1107 (2001).
- <sup>76</sup>Y. Tu and A. Laaksonen, Chem. Phys. Lett. **329**, 283 (2000).